Post-print : Journal of Building Performance Simulation, Volume 9, Issue 6, 2016, p. 663-679

Simple Modelling Procedure for the Indoor Thermal Environment of Highly Insulated Buildings Heated by Wood Stoves

[1]Laurent Georges and [2]Øyvind Skreiberg

[1]Energy and Process Engineering Department, Norwegian University of Science and Technology (NTNU), Trondheim, Norway

Kolbjørn Hejes vei 1b, NO-7491 Trondheim, Norway, laurent.georges@ntnu.no

[2]Department of Thermal Energy, SINTEF Energy Research,

Kolbjørn Hejes vei 1A, 7465 Trondheim, Norway, oyvind.skreiberg@sintef.no

Post-print : Journal of Building Performance Simulation, Volume 9, Issue 6, 2016, p. 663-679

Simple Modelling Procedure for the Indoor Thermal Environment of Highly Insulated Buildings Heated by Wood Stoves

Space heating using wood stoves is a popular solution in many European countries. The nominal power of the state-of-the-art stoves is oversized compared to the needs of highly insulated buildings, leading to a risk of overheating. A modelling procedure is here developed in order to investigate the indoor thermal environment generated by wood stoves in such buildings. This procedure is kept simple to perform all-year detailed dynamic simulations (e.g. using TRNSYS) at an acceptable computational cost. A specific experimental setup has been developed for validation, essentially regarding the interaction between the stove and the building. The largest source of error appears to be the thermal stratification in the room where the stove is placed. The experiments prove that the model gives a fair insight into the global thermal comfort. Therefore, it is possible to investigate the conditions required for a stove to be properly integrated in a highly insulated building.

Keywords: space heating, wood stoves, passive house, thermal comfort

1. Introduction

Wood is a very important renewable energy source. Space heating (SH) using wood stoves is a widespread strategy in many European and Nordic countries. In Norway, wood stoves provide about 20% of the SH needs of the residential building stock and account for about half of the bioenergy use. Norway has also decided to double its use of bioenergy by 2020 (Norwegian Ministry of Petroleum and Energy 2008). In this country, wood stoves represent the second largest source of installed power after hydroelectricity.

A second issue is that energy consumption of buildings in developed countries comprises 20-40% of the total energy use (Pérez-Lombard, Ortiz, and Pout 2008). Thus making reductions here has become a major concern, as illustrated by the European Performance of Building Directive (European Parliament 2010). A common strategy is to reduce the SH needs by a better insulation of the building envelope. Among building concepts that have emerged, the

passive house (PH) is based on a super-insulated building envelope (Feist et al. 2005). Norway has developed its own national definition of the PH standard, the NS 3700 (Standard Norge 2010). Furthermore, the concept of Zero Energy Buildings (ZEB) has also been increasingly popular (e.g. net or nearly ZEB). In many research developments, the PH standard is often considered as a minimal performance requirement for ZEB envelopes, see e.g. (Houlihan Wiberg et al. 2014).

The SH of highly insulated buildings using wood stoves is thus a strategic area. Furthermore, state-of-the-art stoves present acceptable energy conversion efficiency, e.g. 85% (Skreiberg 2012). These stoves can also be used to supplement electric SH and subsequently reduce the peak power in the electricity grid. However, the integration of wood stoves in PH is problematic and it faces two major practical challenges:

(1) First, good indoor air quality (IAQ) and good combustion must be achieved in an airtight building envelope equipped with balanced mechanical ventilation.
(2) Second, the lowest nominal combustion power (P_n) of wood stoves currently available on the market is typically 6-8 kW (Skreiberg 2012). This is well above the SH power of PH (roughly < 3 kW for a detached single-family house located in Oslo during design outdoor conditions). This power oversizing may lead to overheating in the room where the stove is placed or to frequent on-off cycling.

The PH definition is also closely related to the potential to simplify the SH distribution system. It was basically proposed using the air-heating concept (Feist et al. 2005; Georges, Berner, and Mathisen 2014). Therefore, it is also worth investigating how a wood stove can contribute to this simplification and how it distributes heat throughout the entire building envelope.

The present work only focuses on the challenges related to the indoor thermal environment: IAQ is not part of the work. The overall objective here is to investigate the

proper integration of wood stoves in highly insulated buildings using simulation techniques. For instance, simulation can be used to perform quick prototyping of the next stove generation designed for houses with low SH demands, see e.g. (Skreiberg 2011-2014).

Given the current power oversizing of wood stoves, there is essentially no *steady-state* regime in the building: there is no balance between the heat release from the stove and the thermal losses of the building envelope. Consequently, the room temperature where the stove is placed will rise progressively during a combustion cycle. The objective is to limit this temperature increase to an acceptable temperature level. The problem is essentially *dynamic*. The conditions for good integration are linked to the thermal properties of the the stove (e.g. P_n, power modulation range, stove thermal mass) and also to the thermal properties of the building envelope (e.g. its thermal mass, internal door opening) as well as to the boundary conditions of the building (e.g. different climatic zones). In order to develop robust conclusions, *sensitivity analyses* are required for this large set of physical parameters. Furthermore, physical timescales can be as low as ~1min for the stove combustion control, or for the flow through open doorways. On the contrary, highly insulated buildings have a time constant of a few days. In addition, the boundary conditions of the buildings vary significantly throughout the heating season. For instance, the solar and internal gains play a major role in the SH of highly insulated buildings and they are known to vary significantly. Consequently, all-year dynamic simulations with a small time step (~1min) should be performed.

A simple modelling procedure is thus needed in order to give an insight into the all-year thermal comfort at an acceptable computational cost, a cost compatible with sensitivity analyses and short time steps. As the physical problem is closely related to the building thermal dynamics, the modelling procedure should be easily implemented in the main existing building simulation software packages (e.g. TRNSYS, EnergyPlus, IDA-ICE). Using a simple modelling procedure to perform all-year simulations, the critical operating conditions can be

determined. These periods are limited in time and they can be used to perform simulations with a better physical resolution, such as Computational Fluid Dynamics (CFD).

The overall procedure to model a wood stove interacting dynamically with a building can be generically visualized as illustrated in Figure 1. Based on the instantaneous air dry-bulb temperature (T_s) of the room at a given time from the multi-zone building simulation, the combustion power of the stove (P_c) is controlled as a function of the room set-point temperature (T_{set}). A model is then applied for the wood combustion dynamics that ultimately gives the power delivered to the stove envelope as a function of time (P_d). A specific model component then computes the heat transfer within the stove envelope. The instantaneous stove surface temperature (T_{stove}) or the power emitted to the room (P_e) is then obtained. Finally this last quantity is introduced inside the multi-zone building model. Considering this generic framework, the existing developments on wood stove modelling reported in the literature can be categorized. Each of them covers a limited part of the complete modelling chain (see Figure 1):

- Regarding pellets, Persson et al. (2009) developed a model for stoves as well as boilers. It essentially accounts for the stove control, combustion, carbon monoxide (CO) emissions and the heat transfer through the stove envelope. The model explicitly accounts for the start and stop phases of a combustion cycle where the CO emissions are significant. Nevertheless, the modelling of the thermal interaction between the stove surface and the room is limited. This model has been implemented in TRNSYS (TRANSSOLAR 2009) and applied to two simulation cases (Fiedler 2009; Persson 2005).
- Regarding wood log stoves, the combustion cycle should be considered as a batch process. The duration of one combustion cycle has the same order of magnitude as the time scale of the stove and building envelopes. Therefore, the dynamics of the

combustion cycle should be captured accurately. Saastamoinen et al. (2005) and Tuomaala, Simonson, and Piira (2002) introduced models for the heat input and the heat transfer through the envelope of heat-storing stoves. Likewise, Skreiberg (2002) developed a semi-empirical model for the time profile of P_c, see Figure 2, as well as a one-dimensional heat transfer model for lightweight stove envelopes.

- As regards the stove heat released within the building, Ghaddar, Salam, and Ghali (2006) developed a so-called space-heat model that accounts for the heat transfer between stove surfaces and the room. It mainly introduced a method to evaluate the thermal comfort in the presence of a strong non-uniform thermal radiation. Very little is said about the physics inside the stove.
- Considering case studies and applications, detailed dynamic thermal simulations have already been performed in order to determine the conditions required for a stove to be properly integrated in a PH. A single-family detached house typology has been investigated for the temperate climate of Belgium and for Nordic conditions (Georges, Skreiberg, and Novakovic 2013; Georges, Skreiberg, and Novakovic 2014). These conclusions are given for stoves without large heat storage capacity so that they should be considered conservative scenarios. An analogous analysis with similar conclusions was performed by Blumrich et al. (2007) for German PH. Unfortunately, these studies essentially reported on results and did not sufficiently introduce the modelling procedure or the validation.

As regards the stove integration in PH, the modelling procedure should be able to give insight into the thermal comfort in the room where the stove is placed (essentially to investigate the overheating) as well as the heat transfer between rooms (to investigate the temperature difference). First, an acceptable modelling procedure should thus properly capture the interaction between the stove surface and the building. Except for the work of

Ghaddar, Salam, and Ghali (2006), this physical aspect has most often been disregarded. The present paper proposes two possible procedures and validates them by means of experiments. Second, the heat transfer through open doorways should be reproduced accurately in the specific context of natural convection generated by a stove. The usual flow approximation in building models is here compared to experiments. The remainder of the modelling chain, see Figure (1), can be easily taken from the above-mentioned literature (i.e. stove control, combustion, heat transfer in the stove).

The remainder of the paper is organized as follows. The two modelling procedures are introduced in Section 2. They especially differ in the treatment of the thermal radiation from the stove. Both approaches have been implemented in TRNSYS. A specific experimental setup that has been created in order to validate these procedures is described in Section 3. An electric stove has been developed which enables us to mimic the thermal comfort generated by different stove technologies. Practically, it enables testing (or emulating) different stoves and operating conditions in the same building. This electric stove has been used during a measurement campaign in a PH. The time evolution of the temperature field as well as the velocity magnitude within an open doorway have been measured during different stove cycles as reported in Section 4. Simulation results using the two modelling procedures are then compared to measurements and their respective performance discussed in Section 5.

2. Modelling procedures

To limit the computational time and the number of input parameters, the modelling procedures are kept deliberately simple. This was done by adopting a set of reasonable assumptions. The present work focuses on the simplifications done on the physical interaction between the stove surface and the building, as well as the resulting thermal comfort. As already mentioned, the modelling procedures have been implemented in TRNSYS but they can easily be implemented in the other main building simulation tools (e.g. EnergyPlus, IDA-

ICE). For instance, the thermal dynamics of the building is computed using the TRNSYS component termed *Type56b* (TRANSSOLAR 2011, 2009) assuming a uniform air temperature in each thermal zone. At each time step, several sub-iterations are performed between the model components of Figure 1 until the overall system convergences. This is a natural way to formulate and solve multi-domain and multi-physical problems in TRNSYS.

Interaction between the stove and the room

The heat emission from the stove surfaces can be considered in two different ways within the building model, see Figure 3. This essentially influences the way thermal radiation is accounted for during the simulation.

The first and most obvious way is to combine the stove and building geometries and consider the stove surface as any other wall of the room. As the stove is then completely embedded in the building model, this *strongly coupled* approach is the most physical one. Without loss of generality, the different surfaces of the stove can have different temperatures. Nevertheless, it is not obvious that all building simulation programs can support this modelling approach. For instance, view factors should be computed between surfaces in the presence of obstacles. If the stove geometry is complex, it should probably be simplified to be supported by the building simulation program (that usually only considers planes).

Alternatively, heat emitters are often introduced in multi-zone building models as *internal gains*. This is a *loosely coupled* approach as the stove geometry is not physically combined with the building geometry. From one side, the building model only "views" the stove as an internal gain (without knowledge of its geometry). From the other side, the stove only "views" the building as a large isothermal enclosure, with a uniform air temperature, T_s, and uniform mean radiant temperature of wall, $T_{r,mrt}$. The underlying assumptions are:

1. The stove is small compared to the room geometry so that the thermal radiation from the stove to the room is not significantly influenced by the room geometry.

2. The temperature difference between the stove surfaces and the environment is larger than the difference between the surfaces within the room, so that the room is essentially seen as isothermal from the stove.
3. The surface temperature of the stove, T_{stove}, can be assumed uniform.

These important assumptions could still be acceptable in many applications.

The way the stove and the building models are connected is now introduced. In both the strongly and loosely coupled approaches, the power emitted by the stove by convection (P_{ec}) is based on a correlation:

$$P_{ec} = F_c(T_{stove} - T_s) \quad (1),$$

where F_c is an algebraic equation. This correlation can be based on measurements or computed using CFD. P_{ec} is subsequently applied to the zone air-node.

For the loosely coupled approach only, the power emitted by the stove surface by radiation (P_{er}) is evaluated by assuming that the stove is very small compared to the room. Then,

$$P_{er} = \sigma \epsilon F_r(T_{stove}^4 - T_{r,mrt}^4) \quad (2),$$

where σ is the Stefan-Boltzmann constant and ε the emissivity of the stove surface, and, F_r, an algebraic equation. To evaluate thermal radiation, temperatures are expressed in Kelvin. If the stove geometry is convex, then F_r is simply equal to the stove surface (Incropera et al. 2007). P_{er} is subsequently distributed among the walls of the rooms as a function of the view factors (from the stove considered as a point source to the different walls of the room). For the strongly coupled approach, the thermal radiation from the stove surfaces is computed along with the other room surfaces by the building simulation program. In TRNSYS, longwave radiation exchanges are computed using the Gebhart method (TRANSSOLAR 2011; Gebhart 1971).

Finally, like many stoves developed for well-insulated envelopes with balanced mechanical ventilation, the stove is here assumed airtight, extracting its combustion air directly from the outside using a proper air-intake duct. Then, the stove does not use air from the building envelope and does not interact with the balanced mechanical ventilation. In addition, it is here assumed that no particular device is used to increase heat emitted by convection, such as a fan or radiation shields.

As regards the implementation of both approaches in TRNSYS, view factors are evaluated exactly using analytical formula which are only valid if the room geometry is convex (TRANSSOLAR 2011; Schröder and Hanrahan 1993). When rooms are concave (e.g. "L"-shaped), software such as TRNSYS approximate the view factor between the walls in an area-weighted manner. When view factors of concave rooms need to be evaluated accurately (as it is here), they should be pre-computed externally with dedicated numerical tools and subsequently imposed to TRNSYS as input parameters. For instance, the detailed view factors have here been evaluated using the numerical method of Dobrowolski, Giacomet, and Mendes (2007) implemented in Matlab®.

Convective heat transfer between rooms

In PH, the opening of internal doors proved to be an efficient process to exchange heat between rooms (Feist et al. 2005). In order to investigate the natural convection inside the envelope, the airflow between rooms needs to be computed. In theory, there are two types of flow between two rooms connected by a large opening: *bulk density flow* or *boundary layer flow* (Scott, Anderson, and Figliola 1988). They are characterized by the *isothermality factor* defined as the ratio of the air temperature difference between rooms (i.e. the bulk temperature difference) and the wall temperature difference between rooms. Bulk density flow will develop when the isothermal factor is near unity, corresponding to a small temperature

difference between the bulk and wall temperatures. When this difference is large and the isothermal factor decreases to zero, the flow is boundary driven (or motion-pressure-driven flow). In the case of natural convection generated by a stove with high surface temperatures, it is a priori difficult to determine the type of flow regime. We have been unable to find any research that has previously investigated this question.

In the present modelling procedure, the flow between rooms is computed using a ventilation network model (Chen 2009), here using TRNFLOW (TRANSSOLAR 2009) based on the COMIS library. The bi-directional flow through doors is then modelled using a *large opening approximation* which essentially assumes a bulk density flow (Etheridge and Sandberg 1996). The mass flow generated by the bi-directional flow through a door is computed in the following way (TRANSSOLAR 2009):

$$m_{12} = C_d \int_0^H \sqrt{2.\rho_1(z).f_{12}(z)}.w(z).dz \quad (3),$$

$$m_{21} = C_d \int_0^H \sqrt{2.\rho_2(z).f_{21}(z)}.w(z).dz \quad (4),$$

where

- C_d is the discharge coefficient to tune the model to a specific test case. It may typically range from 0.4 to 0.8 (Heiselberg 2006; Etheridge and Sandberg 1996),
- z is the vertical direction and H, the height of the doorway,
- subscript 1 refers to the warm zone (typically, a living room),
- subscript 2 refers to the cold zone (typically, a staircase),
- m_{12} refers to the mass flow from zone 1 to zone 2,
- m_{21} refers to the mass flow from zone 2 to zone 1,
- $f_{12}(z)$ is equal to $p_1(z)$-$p_2(z)$ if positive, or is equal to zero,
- $f_{21}(z)$ is equal to $p_2(z)$-$p_1(z)$ if positive, or is equal to zero,

- w(z) is the width of the door.

The pressure $p_i(z)$, with subscript i equalling 1 or 2, is evaluated based on the reservoir (or bulk) conditions on both sides of the doorway:

$$p_i(z) = p_i(0) - \int_0^z \rho_i(\tau).g.d\tau \quad (5),$$

where g is the gravity acceleration and $p_i(0)$ the reference pressure of zone i. This last value is computed to get the conservation of mass throughout the ventilation network. The convective heat transfer between both zones can be expressed as

$$h_{12} = C_d \int_0^H \sqrt{2.\rho_1(z).f_{12}(z)}.C_p.T_{s,1}(z).w(z).dz \quad (6),$$

$$h_{21} = C_d \int_0^H \sqrt{2.\rho_2(z).f_{21}(z)}.C_p.T_{s,2}(z).w(z).dz \quad (7),$$

where

- $T_{s,i}(z)$ is the vertical air temperature field in zone i,
- C_p is the air specific heat capacity,
- h_{12} refers to the convective heat transfer from zone 1 to zone 2,
- h_{21} refers to the convective heat transfer from zone 2 to zone 1.

As the air temperature field is assumed uniform in the building model, $T_i(z)$ and $\rho_i(z)$ are then not dependent on the vertical direction, z.

Thermal comfort evaluation

The overall thermal comfort is evaluated using the thermal balance approach of Fanger (1967) assuming the body as a whole, here using the ISO 7730 (CEN 2005). The comfort diagnostic is mainly done using the operative temperature (T_{op}) based on T_s and the mean radiant

temperature ($T_{c,mrt}$) (from the occupant point of view). This last temperature requires computing the detailed view factors from the occupant location to the different surfaces of the room. In the strongly coupled approach, the computed $T_{c,mrt}$ takes by definition the stove surface temperature into account (T_{stove}). In the loosely coupled approach, the stove geometry is not present as the stove is considered a point source radiative gain. If the occupant is located far from the stove, the mean radiant temperature computed by the building model ($T_{c,mrt,sim}$) can nonetheless be corrected to account for the stove surface temperature:

$$T_{c,mrt} \cong \sqrt[4]{(1 - F_s)\, T_{c,mrt,sim}^4 + F_s\, T_{stove}^4} \qquad (8),$$

where F_s is the view factor of the stove from the occupant point of view.

As a simplified approach, local thermal discomfort is not taken into account. The building model is not able to provide for the local air velocity inside the room so that the draught effect cannot be investigated. Furthermore, the air in each room in the building is being considered as fully mixed and isothermal so that the vertical thermal stratification is by definition not captured (Wang and Chen 2008). In fact, it is possible to define several vertical air nodes for a given thermal zone within most of the existing building simulation tools. Nevertheless, the convective coupling between each layer must be known, for instance generated by the thermal plume of the stove or the downward boundary layers along the external walls. These quantities are not known a priori and are not expected to be computed correctly in the present modelling framework. Furthermore, most of the existing multi-layer air models implemented in the main building simulation packages have been developed for other applications, such as displacement ventilation, so that they cannot be directly applied for the present case, see e.g. for EnergyPlus (DOE 2014). Note that some software packages, such as IDA-ICE (Eriksson et al. 2012) are currently developing room models that could potentially evaluate the stratification properly. Nevertheless, it is reasonable to assume that

the fully mixed air is representative of the current capabilities of most building simulation tools.

Finally, the effect of radiation asymmetry is also neglected. It is in fact possible to evaluate opposite plane radiant temperatures (T_{pr}) using the building model (i.e. the surface temperatures and the geometry). Nevertheless, the thermal comfort criterion of ISO 7730 for radiation asymmetry is established for large plane surfaces with a maximal T_{pr} difference of 35°C. It is thus questionable to apply this criterion to a point source, such as a stove, with relatively high surface temperatures (e.g. >100°C). In this context, Ghali, Ghaddar, and Salloum (2008) investigated the effect of the asymmetric radiation field from a stove on the thermal comfort using a multi-segmented bioheat model. Their study suggested that far from the stove, the thermal comfort can be evaluated globally and the effect of radiation asymmetry be neglected.

3. Movable electric stove

In order to validate the modelling procedure, an experimental campaign was needed. The main issue was to find PH in Norway that was already equipped with wood stoves. To our knowledge, most Norwegian PH have so far been equipped with hydro-stoves that deliver a significant part of the P_c to a water jacket (and subsequently to a storage tank and a hydronic system). This was not really relevant for our investigations as the heat directly emitted to the room is then limited to 1-3 kW. Furthermore, it is rather difficult to accurately evaluate the power emitted (P_e) by the stove envelope during real stove operation. It would be difficult to make a direct relation between the heat release of the stove and the resulting thermal comfort. For these reasons, it was decided to build an electric stove that mimics the thermal environment generated by a real one. In addition, this makes it possible to install the system in any PH disregarding the presence of a chimney and avoiding problems with the IAQ (e.g. pollution by small particles).

The layout of the experimental setup is shown in Figure 4. The movable electric stove, with a 15.5 kW maximum power, is a box with sides of 0.60 m and a height of 1.20 m. It consists of 9 heating plates where a flexible and distributed electric resistance has been fastened on their back sides: 2 plates per vertical face and 1 plate on the top. The back side of the heating plates is then further insulated with 10 cm mineral wool that can withstand high temperatures. Thus the inner stove structure stores almost no heat: the electric power is delivered to the plate and subsequently is emitted to the room. The plates are made in aluminium to ensure a uniform temperature distribution on the surface. Their thickness has been limited to 3 mm to get a quick response time from the stove surface temperatures. Finally, the plates have been covered by a layer of special stove paint in order to get the correct emissivity, ε. This black paint emissivity was calibrated at 0.9 using an infrared (IR) camera. In practice, 3 surface temperatures are controlled independently while the 6 remaining surface temperatures are controlled in pairs of 2 surfaces. Hence, 6 independent set-point temperatures can be found on the movable stove surfaces. This has been done so as to mimic stoves that have uneven surface temperatures during operation. Further work needs to be performed to investigate whether the electric stove enables the emulation of the power directly emitted by the combustion chamber through a stove window. The 6 currents in the 9 resistances are modulated using thyristors which are controlled to enforce the 6 input set-point surface temperatures. The instantaneous surface temperatures are measured using thermocouples and transferred to a computer equipped with LabVIEW. A PID control is implemented in this program to evaluate the control signal for the thyristors. Profiles of the set-point surface temperatures are given as input. These time profiles have been here provided by the batch combustion model of SINTEF Energy Research (Skreiberg 2002), but other sources, such as measurements, can be used. In the present validation case, the same temperature profile is imposed on all the electric stove surfaces.

This movable electric stove enables to mimic the thermal environment generated by different stove technologies in the same building, for instance having different P_n, batch load, power modulation and heat storage capabilities. Only the shape of the stove cannot be changed: this parameter mainly influences the ratio between convected and radiated power emitted to the room (i.e. P_{ec}/P_{er}).

At first, laboratory measurements were done on the stove to prove that it operates correctly and safely. They clearly demonstrated that the heat release of the electric resistance is well distributed along the plate and gives rather uniform surface temperatures (i.e. < 10°C difference). This has been verified using an IR camera giving images such as in Figure 5. The stove has almost no thermal bridges so that all the heat emitted to the room originates from the stove plates. Furthermore, the heat exchange between the stove heating plates and the feet is negligible, which enables it to operate safely in a building.

The correlation for convection, Eq. (1), and the relation for thermal radiation, Eq. (2), can be now established for this specific stove geometry. The power emitted by the stove surface by convection (P_{ec}) is obtained using the well-known Churchill and Chu (1975) correlation for laminar and turbulent flows over an isothermal plate. Given the range of T_s and usual characteristic lengths considered for stoves, the correlation is further simplified into:

$$P_{ec} = 1.22A(T_{stove} - T_s)^{4/3} \quad (9),$$

where A is the stove external area. As regards the thermal radiation in the loosely coupled approach, the electric stove is a small convex geometry in a large enclosure giving the simple equation (Incropera et al. 2007):

$$P_{er} = \sigma A \epsilon (T_{stove}^4 - T_{mrt,r}^4) \quad (10),$$

The modelling approximation between P_e and T_{stove} has also been tested in a large room in the lab. The results are reported in Figure 6, where the heat released to the room has been

obtained experimentally by measuring the delivered electricity to the stove during steady-state conditions. Two methodologies have been employed to measure the delivered electrical power: using a current measurement (#1) and the output signal of the thyristors (#2). In both cases, Eqs. (9) and (10) combined together were found to give accurate results. Finally, the T_{stove} is imposed by the electric stove control, so this relationship is also important to know the exact corresponding emitted power (P_e) to the room.

4. Experimental setup in the Passive House

The electric stove was placed in a PH in Trondheim during the months of March and April 2014. This is a terraced house in the MiljøGranåsen project, which is currently the largest PH construction project in Nordic countries. It will consist of 430 dwelling units with a total heated area of 34 000 m². MiljøGranåsen is developed by Heimdal Bolig and is also part of the EBLE, Concerto and Eco-city research projects. During the measurement campaign, the PH was unoccupied and unfurnished. It consists of three storeys as shown in Figure 7.

The building is a timber construction except for the basement that is in concrete. In that respect, the building thermal mass may be characterized as *very-light* or *light* (CEN 2008). The heated area is 142.5 m². The U-value of the external walls is 0.15 W/m².K while the different triple-glazed windows have an overall U-value between 0.7 and 0.85 W/m².K. The roof has a thermal transmittance of 0.06 W/m².K. The equivalent U-value of the basement floor is 0.1 W/m².K while the basement walls have an equivalent U-value of 0.19 W/m².K. The movable stove was placed in the living room on the ground floor. The hygienic ventilation has an air change rate (ach) of 0.52. The heat recovery (HR) unit of the balanced mechanical ventilation has a rated temperature efficiency (EN 308) of 88% while an electric resistance further preheats the fresh air to 19°C. A net air mass flow of 33 m^3/h is moving downwards from the first floor to the ground floor through the open staircase. The SH needs

are evaluated at 17.1 kWh/m².year using two Norwegian standards (Standard Norge 2007, 2010).

The house has then been instrumented to monitor the thermal environment during the stove operation, see Table 1 and Figure 8.

As regards the local temperature distribution on the ground floor, the thermal stratification has been measured by five PT-100 sensors distributed on a vertical rod from the floor to the ceiling level. One bar is located in the middle of the ground floor near the kitchen while a second bar is positioned in the open staircase. In the middle of the kitchen and the living room areas, a radiant temperature transducer and a PT-100 probe which measures the air dry-bulb temperature (T_s) are placed 0.8 m above the ground. Given the ground floor layout, these probes are located opposite in the room. The horizontal air temperature distribution can then be checked. Using the same location in the kitchen, the operative temperature (T_{op}) is measured using a black globe. Five PT-100 temperature sensors are taped to different walls to have an approximation of the temperature difference between the walls. For half of the test cases, the airflow in the doorway between the ground and first floor has been measured using a vertical pole located in the middle of the door mounted with ten omni-directional air velocity transducers (TSI 8475) and ten thermocouples of type T. Basically, the building has a large open staircase which would have made the measurement of velocities difficult (i.e. very low velocity magnitude < 0.1 m/s). It was decided to screen part of the staircase with thermally insulated plates to leave a single opening of 2.35 m x 0.9 m that should represent a door. For each of these probes, data were registered every minute.

As regards the temperature distribution between rooms, eleven temperature loggers were placed in the building. In addition, three loggers measured the temperature of the ventilation inlet air before and after the heat recovery unit, as well as after the pre-heating battery. These data loggers registered the temperature every fifteen minutes.

Finally, the outdoor air temperature was also registered every fifteen minutes in a sheltered place. The direct and total solar irradiation on a horizontal plane were recorded every minute by a weather station located 3.5 km away from the monitored PH.

In total, twelve different stove cycles have been tested, see Tables 2 and 3. They were taken to be representative of the performance of state-of-the-art stoves available on the market. For the pellet stoves, P_n of 6 kW and 8 kW have been tested during combustion cycles of 90 min along with stove thermal masses (I_{th}) of 50 kJ/K and 150 kJ/K and with a constant power modulation of 30% as well as without modulation. Only four cases were tested. For the log stoves, P_n of 4 kW and 8 kW were tested for batch loads of 5 kWh nd 10 kWh along with stove thermal masses of 50 kJ/K and 150 kJ/K and with a constant power modulation of 50% as well as without modulation. The time profiles of T_{stove} have been generated using the batch load model of Skreiberg (2002) and are taken to be equivalent to the case study of Georges, Skreiberg, and Novakovic (2014). The measurement campaign was performed between 19 March and 10 April 2014. During this period of time, the weather was unusually mild in Norway including in the Trondheim area. It resulted in outdoor temperatures (T_{ext}) between -1°C and 8°C, giving a low space-heating demand.

For the twelve test cases, the following indicators are monitored: the maximal operative temperature increase during a cycle ($\mathbf{\Delta}T_{op,max}$) in the kitchen at 0.8 m height, the maximal air temperature difference in an horizontal plane at 0.8 m above the ground floor ($\Delta T_{s,hor,max}$), the maximal air temperature difference from floor to ceiling on the ground floor ($\Delta T_{s,vert,z1,max}$) and the maximal air temperature difference from the ground floor to the first floor ceiling measured in the staircase ($\Delta T_{s,vert,z2,max}$). Measurements are reported in Table 4 where a distinction has been made between cases with a large direct solar irradiation and cases with overcast sky. In fact, the direct solar radiation affected the sensors placed in the living room area. Finally, each test case has been started when the PH operative temperature

was stabilized at ~21°C. It means that after each test case, a waiting period was applied until the building cooled down to ~21°C. Given the long time constant of PH, this period ranged from a couple of hours to one day. For the test cases n°2w, 4w and 3p, it turns out that this waiting period was taken too short so that the previous test case was still influencing the following one. Consequently, these three cases have not been considered for the analysis.

5. Results and discussion

Isothermal approximation

For the building model (e.g. Type56) or the ventilation network model to be valid (e.g. TRNFLOW), a set of assumptions must be fulfilled. The main assumption is that the air temperature field in each room can be simplified into a single air temperature (Wang and Chen 2008; Chen 2009), sometimes called air-node (i.e. a well-stirred tank approximation).

Without large solar gains, the air temperature difference between the living room and the kitchen can be properly compared using the $\Delta T_{s,hor,max}$, see Table 4. The temperature field proved to be relatively uniform in the horizontal direction (i.e. lower than 1°C). This is partly due to the flat floor and ceiling (Blomqvist 2009) which enables gravity currents to propagate freely in the horizontal direction. With the presence of obstacles, conclusions could have been different.

On the contrary, the vertical temperature stratification on the ground floor is significant, see $\Delta T_{s,vert,z1,max}$. The higher the power and energy delivered to the room, the higher the stratification. The thermal stratification is in fact the largest source of discrepancy between the well-stirred tank approximation and reality. In the worst cases, the stratification is so large that it should also be accounted for in the evaluation of the local thermal comfort. According to ISO 7730, it should be done by comparing the air temperature difference between head and ankle heights. Except for the test case 6w, this temperature difference for a

person sitting (between 0.1 and 1.1 m height) is lower than 3°C which leads to a thermal environment of category B according to ISO 7730. If the person is assumed standing (between 0.1 and 1.7 m height), many test cases lead to a temperature difference between head and ankle larger than 3°C.

Non-uniform thermal radiation

While the horizontal air temperature difference is small, the wall temperature is significantly influenced by the distance from the stove. Five wall sensors were placed on the ground floor with three attached to walls close to the stove and one to an external wall of the kitchen. It is difficult the measure the space-averaged wall temperatures but, based on these punctual values, a difference of ~5°C may be found. This is also confirmed using the radiant temperature transducer, showing a significant plane radiant temperature (T_{pr}) difference between the kitchen and the living room, see Table 5. It clearly demonstrates the importance of using accurate view factors when distributing the stove internal gains into the room model, as well as when evaluating the resulting thermal comfort for a building occupant. As already mentioned, this step can be critical for many usual building simulation tools as they can only compute the accurate view factors for convex room geometries (where view factors can be evaluated analytically). . As regards the room geometry, an additional constraint for simulation is that each wall should be subdivided in sections of maximum ~3m wide to enable the wall temperature to vary within the room.

Large opening approximation

It is worth investigating whether the ventilation network approach along with the large opening approximation is able to correctly reproduce the airflow through the open doorway.

The thermal plume of the stove is well-mixed in the room as shown by the limited horizontal temperature differences as well as using complementary smoke visualizations.

There is no evidence that the cross-flow in the doorway interacts with the stove plume. Moving the measurement pole along the door width also proved that the flow is essentially one-dimensional (i.e. in the vertical direction). It consistently confirms the assumption of *bulk density flow*. Furthermore, the measured time-averaged velocity is close to the theoretical velocity profile obtained by the large opening approximation, see for example Figure 9. In this case, the discharge coefficient C_{dv} has been evaluated to minimize the error with the measured velocities using a least-squares approach. This coefficient is reported in Table 6 for all the test cases where the velocity was measured properly in the doorway. For all cases, this coefficient ranges between 0.36 and 0.41 and thus appears constant as well as fits within the typical range of [0.4;0.8] reported in the literature.

As regards building simulation, it is more generally relevant to calibrate the discharge coefficient using the mass flow rate. One can distinguish between the coefficient obtained if the thermal stratification is known on both sides of the door (C_{dm}) and the coefficient assuming that both rooms are isothermal (C_{dms}). Their magnitudes are rather similar, meaning that the isothermal approximation does not lead to a large error in the mass flow. This is a known conclusion already reported in IEA EBC Annex 20 (Allard et al. 1992).

In our specific application dealing with temperature differences between rooms, the convective heat exchange is more relevant than the mass flow. This convective heat exchange is known to be significantly affected by the vertical temperature stratification (Allard et al. 1992), see Eqs. (6) and (7). If the stratification is known, the convective heat exchange can be evaluated properly using the same discharge coefficient, C_{dm}. If stratification is not known, one could tune the discharge coefficient to make the large opening model coupling two isothermal rooms fit measurements (C_{des}). In that case, one should increase the coefficient to 0.53-0.62.

As a conclusion, the large opening approximation connecting two isothermal rooms gives a fair approximation of the mass flow. Nevertheless, as the temperature stratification is neglected, a significant error should be expected for the convective heat exchange between rooms (here an underestimation of 30-50%). In a general context, C_d depends significantly on the building geometry. If not known, it is therefore important to simulate the temperature distribution in buildings using a large range of C_d values, such as [0.4;0.8].

Overall model performance

For each of the modelling hypotheses being tested, the overall model performance can be now investigated and discussed. The T_s, $T_{c,mrt}$ and T_{op} have been computed using the described modelling procedure and compared to experiments. The building has been simulated using the exact building geometry and construction materials. Furthermore, the boundary conditions for the building model (i.e. T_{ext} and solar irradiation) have been taken from field measurements. The building is simulated several days before each cycle in order to generate a realistic initial condition comparable to measurements. Conclusions are based on all test cases but are only illustrated using test cases n°5w and 1w in Figures 10 and 11, respectively.

Case n°5w is an 8 kW stove operated at 50% of P_n. The corresponding stove surface temperature (T_{stove}) is reported in Figure 10.a. A large temperature stratification has been measured in the kitchen as reported in Figure 10.b. The mean value (i.e. vertically averaged) can be compared with the isothermal value from simulation. One can notice that the curves do not match in amplitude and phase. In reality, the thermal plume of the stove injects hot air in the upper air layer of the room. This hot air then spreads in a horizontal direction as gravity currents (Blomqvist 2009) and is finally cooled down along the walls to be injected at a lower temperature in the lowest air layers. This mechanism is the basis of the thermal stratification phenomenon and explains the time delay of temperature increase between the upper air layers

near the ceiling and the lower air layers near the floor. By definition, the building model neglects this effect and the convective heat release from the stove (P_{ec}) is directly injected into the single air-node. Therefore, the T_s from the simulation tends to be synchronized with the temperature of the upper air layer from measurements (both with a short delay compared to T_{stove}). Given the large stratification, the simulated T_s should in theory mimic the vertically averaged T_s from measurements. In practice, the increase of T_s computed by simulation always appears very close to the measured T_s at 0.9 m height, a value which is always slightly lower than for the vertically averaged T_s. A similar but less pronounced behaviour can be observed for the case n°1w of a 4 kW stove operated at 50%.

The computed $T_{c,mrt}$ at 0.8m in the kitchen appears to be in very good agreement with measurements, as shown in Figures 10.c and 11.c. This performance would not have been reached without computing the accurate view factors, for instance by only applying area-averaged view factors (results not reported here). The strongly coupled approach performs best. For the loosely coupled approach, a distinction is also made between the $T_{c,mrt}$ computed with and without taking the stove surface temperature (T_{stove}) into account, see Eq. (8). In all cases, including T_{stove} in the $T_{c,mrt}$ evaluation improves results: the higher the T_{stove}, the better the improvement.

Finally, the T_{op} at 0.8 in the kitchen is analysed using Figures 10.d and 11.d.. As T_{op} is taken as the average between the T_s and T_{mrt} and as the simulated T_s is close to the measured air temperature at 0.9 m height, it is thus not surprising to note that simulation is able to fairly simulate the T_{op} at 0.8 m height. As for T_s, a time delay is present but the magnitude is correct. This was confirmed for all test cases as illustrated by the $\Delta T_{op,max}$ in Table 4. For both the strongly and loosely coupled approaches, the agreement between simulation and measurements is remarkable given the simplicity of the model and the complexity of calibration with field measurements.

6. Conclusions

Wood stoves are popular space-heating solutions in many European countries. Nevertheless, nominal power of the state-of-the-art products on the market is oversized compared to the needs of highly insulated building envelopes. In this respect, two simple modelling procedures have been proposed in order to investigate the all-year global thermal comfort at an acceptable computational cost, based on existing building simulation tools. These procedures essentially focus on the interaction between the stove and the building and should be considered as the lowest acceptable resolution to capture this interaction properly. The first approach is *strongly coupled* where the stove geometry is directly integrated within the building model. The second approach is *loosely coupled*, meaning that the stove geometry is not integrated in the building model but rather considered as a convective and radiative internal gain. This assumption is essentially valid when the stove surfaces can be considered isothermal and small compared to the room dimensions. Using these procedures, critical operating conditions and periods during a heating season can be detected. If required, a more detailed modelling approach can then be applied in these critical periods, such as CFD.

A specific experimental setup has been developed to validate these modelling approaches. An electric stove has been developed in order to emulate the thermal comfort generated by different stove technologies. Experiments using isothermal stove surfaces prove that the modelling procedures give a fair insight into the global thermal comfort.

Both procedures are based on a same hypothesis of isothermal room air. In practice, the thermal stratification in the room where the stove is placed appears to be the largest source of error. This can simultaneously affect the conductive heat transfer between rooms, the local thermal comfort sensation as well as the convective heat exchange by flows through open doorways. Nevertheless, this last effect can be limited in simulations by performing a sensitivity analysis on the discharge coefficient of the door (C_d), measurements having shown

that the bulk density flow assumption is appropriate to model this flow. The mean radiant temperature is well reproduced by both modelling procedures, even though the strong coupling is more accurate by definition and has a more general formulation. As a result, the operative temperature is fairly well reproduced by both modelling approaches.

As future work, the model will be further validated: the thermal comfort using the movable electric stove will be tested in other passive houses, presenting other typologies (e.g. detached houses, apartments) as well as during colder periods of the heating season. Furthermore, the modelling procedure will be analysed for stoves with significant differences in surface temperatures. For instance, the modelling of the radiation from the glass door should be carefully discussed. In that respect, it is also necessary to prove that the electric stove is able to correctly emulate the effect of the glass door. In such highly insulated buildings, the thermal losses from the chimney could also affect the comfort, an aspect that also deserves investigation. Finally, the model and measurements will also be compared with other simulation techniques, such as zonal models (Megri and Haghighat 2007) or Computational Fluid Dynamics (CFD), which have the capacity to better capture thermal stratification.

Acknowledgements

The authors would like to acknowledge the Research Council of Norway for its support as this work was performed within the Norwegian research centre for Zero Emission Buildings (ZEB) as well as within the WoodCFD project. Industry partners financing both projects are also acknowledged.

Nomenclature

C_d = discharge coefficient for the bidirectional flow in a doorway

$C_{d,v}$ = C_d tuned to match the velocity profile

$C_{d,m}$ = C_d tuned to match the mass flow

$C_{d,ms}$ = $C_{d,m}$ but assuming two isothermal rooms on both sides of the door

$C_{d,es}$ = C_d tuned to match the convective heat exchange between rooms assumed isothermal

C_p = specific heat capacity of air

ε = stove surface emissivity

σ = Stefan-Boltzmann constant

F_s = view factor of the stove from the occupant locationh_{12}

= convective heat transfer from the warm to the cold room

h_{21} = convective heat transfer from the cold room to the warm room

I_{th} = thermal mass of the stove envelope in [kJ/K]

m_{12} = mass flow from the warm to the cold room

m_{21} = mass flow from the cold room to the warm room

P_n = nominal combustion power of the stove

P_c = instantaneous combustion power of the stove

P_d = power delivered to the stove envelope

P_e = power emitted to the room

P_{ec} = power emitted to the room by convection

P_{er} = power emitted to the room by radiation

T_s = air dry-bulb temperature

T_{op} = operative temperature at the occupant location

T_{set} = set-point air temperature for the room

T_{ext} = outdoor air dry bulb temperature

$T_{r,mrt}$ = mean radiant temperature of the room seen by the stove

$T_{c,mrt}$ = mean radiant temperature of the room and stove, seen by the occupant

T_{pr} = plane radiant temperature

T_{stove} = instantaneous stove surface temperature

$\Delta T_{op,max}$ = maximal T_{op} increase in kitchen during a stove cycle

$\Delta T_{s,hor,max}$ = maximal horizontal T_s difference in ground floor during a stove cycle

$\Delta T_{s,vert,z1,max}$ = maximal vertical T_s difference in living room during a stove cycle

$\Delta T_{s,vert,z2,max}$ = maximal vertical T_s difference in staircase during a stove cycle

References

Allard, F., D. Bienfait, F. Haghighat, G. Liébecq, K van der Maas, R. Pelletret, L. Vandaele, and R. Walker. 1992. "Air flow through Large Opening in Buildings." International Energy Agency.

Blomqvist, C. 2009. "Distribution of Ventilation Air and Heat by Buyoncy Forces Inside Buildings." PhD thesis, Royal Institute of Technology (KTH).

Blumrich, F., W. Feist, W. Hasper, H. Krause, J. Nitsch, R. Pfluger, and R. Strauss. 2007. "Protokollband nr. 36: heizung mit biobrennstoffen für passivhäuser." Darmstadt: Passivhaus Institut.

CEN. 2005. "EN ISO 7730 : Ergonomics of the thermal environment: analytical determination and interpretation of thermal comfort using calculation of the PMV and PPD indices and local comfort criteria." European Committee for Standardization.

CEN. 2008. "EN ISO 13790-2008 : Energy performance of buildings, calculation of energy use for space-heating and cooling." European Committee for Standardization.

Chen, Q. 2009. "Ventilation performance prediction for buildings: a method overview and recent applications." *Building and Environment* 44:848-58.

Churchill, S., and H. Chu. 1975. "Correlating equations for laminar and turbulent free convection from a vectical plate." *International Journal of Heat and Mass Transfer* 18:1323-9.

Dobrowolski, L., B. Giacomet, and N. Mendes. 2007. Numerical Method for Calculating View Factor between Two Surfaces. Paper presented at the Building Simulation 2007, Beijing, China.

DOE. 2014. "EnergyPlus Engineering Reference." U.S. Department of Energy.

Eriksson, L. , G. Grozman, P. Grozman, P. Sahlin, M.H. Vorre, and L. Ålenius. 2012. CFD-free, Efficient, micro indoor climate prediction in buildings. Paper presented at the BSO 2012 conference, Loughborough.

Etheridge, D., and M. Sandberg. 1996. *Building ventilation: theory and measurements*. New Jersey: John Wiley and Sons.

European Parliament. 2010. "Directive 2010/31/EU of the European Parliament and the Council of 19th May 2010 on the energy performance of buildings (recast)." *Official Journal of European Union*.

Fanger, P.O. 1967. "Calculation of thermal comfort: introduction of a basic comfort equation." *ASHRAE Transactions* 73 (2).

Feist, W., J. Schnieders, V. Dorer, and A. Haas. 2005. "Re-inventing air heating: convenient and comfortable within the frame of the Passive house concept." *Energy and Buildings* 37:1186-203.

Fiedler, F., Persson, T. 2009. "Carbon monoxide emissions and combined pellet and solar heating systems." *Applied Energy* 86:135-43.

Gebhart, B. 1971. *Heat Transfer*. New York: McGraw-Hill.

Georges, L., M. Berner, and H.M. Mathisen. 2014. "Air heating of passive houses in cold climate: investigation using detailed dynamic simulations." *Building and Environment* 74:1-12.

Georges, L., Ø. Skreiberg, and V. Novakovic. 2013. "On the proper integration of wood stoves in passive houses: investigation using detailed dynamic simulations." *Energy and Buildings* 59:203-13. doi: 10.1016/j.enbuild.2012.12.034.

Georges, L., Ø. Skreiberg, and V. Novakovic. 2014. "On the proper integration of wood stoves in passve houses under cold climates." *Energy and Buildings* 72:87-95.
Ghaddar, N., M. Salam, and K. Ghali. 2006. "Steady thermal comfort by radiant heat transfer: the impact of the heater position." *Heat Transfer Engineering* 27 (7):29-40.
Ghali, K., N. Ghaddar, and M. Salloum. 2008. "Effect of stove asymmetric radiation field on thermal comfort using a multisegmented bioheat model." *Building and Environment* 43:1241-9.
Heiselberg, P. 2006. "Modelling of natural and hybrid ventilation." Aalborg University.
Houlihan Wiberg, A., L. Georges, T.H. Dokka, M. Haase, B. Time, A.G. Lien, S. Mellegård, and M. Maltha. 2014. "A net zero emission concept analysis of a single-family house." *Energy and Buildings* 74:101-10.
Incropera, F., D. Dewitt, T. Bergman, and A. Lavine. 2007. *Fundamental of heat and mass transfer*. 6th ed. New Jersey: John Wiley and Sons.
Megri, A.C., and F. Haghighat. 2007. "Zonal Modeling for Simulating Indoor Environment of Buildings: Review, Recent Developments, and Applications." *HVAC&R research* 13 (6):887-905.
Norwegian Ministry of Petroleum and Energy. 2008. "Strategi for økt utbygging av bioenergi." Norwegian Ministery of Petroleum and Energy.
Pérez-Lombard, L., J. Ortiz, and C. Pout. 2008. "A review on buildings energy consumption information." *Energy and Buildings* 40:394-8.
Persson, T., F. Fiedler, S. Nordlander, C. Bales, and J. Paavilainen. 2009. "Validation of a dynamic model for wood pellet boilers and stoves." *Applied Energy* 86:645-56.
Persson, T., Norlander, S., Rönnelid, M. 2005. "Electrical savings by use of wood pellets stoves and solar heating systems in electrically heated single-familly houses." *Energy and Buildings* 37:920-9.
Saastamoinen, J., P. Tuomaala, T. Paloposki, and K. Klobut. 2005. "Simplified dynamic model for heat input and output of heat storing stoves." *Applied Thermal Engineering* 25:2878-90.
Schröder, P., and P. Hanrahan. 1993. On the Form Factor between Two Polygons. Paper presented at the 20th Annual Conference on Computer Graphics and Interactive Techniques.
Scott, D., R. Anderson, and R. Figliola. 1988. "Blockage of Natural Convection Boundary Layer Flow in a Multizone Enclosure." *International Journal of Heat and Fluid Flow* 9 (2):208-14.
Skreiberg, Ø. 2002. "Fuelsim-Transient: a mass, volume and energy balance spreadsheet for batch combustion applications." Trondheim: NTNU.
Skreiberg, Ø. "StableWood: new solutions and technologies for heating of buildings with low heating demand." SINTEF. http://www.sintef.no/Projectweb/StableWood/.
Skreiberg, Ø., Seljekog, M., Karlsvik, E. 2012. Environmental and energetic performance history and further improvement potential for wood stoves. Paper presented at the 20th European Biomass Conference and Exhibition, Milan.
Standard Norge. 2007. "NS 3031:2007 Calculation of energy performance of buildings, methods and data."
Standard Norge. 2010. "NS 3700:2010 Criteria for passive houses and low energy houses (residential buildings)."
TRANSSOLAR. 2009. "TRNFLOW: a module of an air flow network for coupled simulation with TYPE 56 (multi-zone building of TRNSYS)."
TRANSSOLAR. 2011. "TRNSYS 17: Volume 5, Multizone Building modeling with Type56 and TRNBuild."

Tuomaala, P., C. Simonson, and K. Piira. 2002. "Validation of Coupled Airflow and Heat Transfer Routines in a Building Simulation Tool." *ASHRAE Transactions* 108 (1):435-49.

Wang, L., and Q. Chen. 2008. "Evaluation of some assumptions used in multizone airflow network models." *Building and Environment* 43 (10):1671-7.

Table 1. List of measurement probes.

Type	Number	Location	Precision	Measure	Freq.
PT-100	5	Ground floor	±0.1°C	Ts, stratification	1 min
	5	Staircase	±0.1°C	Ts, stratification	
	1	Living room	±0.1°C	Ts, 0.8 m height	
	1	Kitchen	±0.1°C	Ts, 0.8 m height	
	1	Kitchen	±0.1°C	Top, 0.8 m height	
	5	Walls	±1°C	Twall	
Radiant temperature transducer INNOVA MM0036	1	Living room and kitchen	±0.5°C	Tc,mrt, 0.8 m height	Manual
Thermocouples Type T	10	Doorway or Living room	±1% ±0.5°C	Ts, profile or stratification	1 min
Anemometer TSI 8475	10	Doorway	±3% ±0.005 m/s	Air velocity profile	1 min
Temperature logger iButton Maxim Integrated DS1922L	11	Each room	±0.5°C	Ts, one by room	15 min
	1	Outdoor	±0.5°C	Ts, sheltered	
	3	Air Handling Unit	±0.5°C	Ts fresh air	

Table 2. Matrix of test cases that emulate pellet stoves.

Case	Pn	Modulation	Ith	Cycle length
N°	[kW]	[% of Pn]	[kJ/K]	[min]
1p	6	100	50	90
2p	6	100	150	90
3p	8	30	50	90
4p	8	100	150	90

Table 3. Matrix of test cases that emulate wood log stoves.

Case	Pn	Modulation	Ith	Batch load
N°	[kW]	[% of Pn]	[kJ/K]	[kWh]
1w	4	50	50	5
2w	4	100	50	5
3w	4	50	50	10
4w	4	100	50	10
5w	8	50	50	10
6w	8	100	50	10
7w	8	50	150	10
8w	8	100	150	10

Table 4. Maximal temperature differences during each stove cycle during experiments (Exp), using strongly coupled (Strong) and loosely coupled (Loose) approaches.

Case	Sun	Text	ΔTs,hor,max	ΔTs,vert,z1, max	ΔTs,vert,z2, max	ΔTop,max		
		Outside	Ground floor	Ground floor	Staircase	Kitchen		
		Exp	Exp	Exp	Exp	Exp	Strong	Loose
N°	[Yes-No]	[°C]	[°C]	[°C]	[°C]	[°C]	[°C]	[°C]
1p	No	-1	0.2	11	4.1	4.6	4.8	4.6
2p	No	+8	0.5	8.1	2.0	3.3	3.2	3.2
4p	No	+5	1.4	11	5.3	4.5	4.9	4.7
5w	No	+5	0.3	9.3	5.1	4.7	4.6	4.6
7w	No	+5	0.4	7.6	4.2	4.0	4.3	4.3
8w	No	+7	0.8	8.9	3.6	4.8	5.4	5.3
1w	Yes	+4	3.5	4.3	3.7	3.8	3.9	3.9
3w	Yes	+4	4.6	6.7	7.1	6.6	6.4	6.4
6w	Yes	+4	4.5	13	7.8	6.0	7.4	7.1

Table 5. Measured radiation asymmetry at the end of each stove cycle, only reported for test cases during overcast sky ($T_{pr,front}$ and $T_{pr,back}$ are the plane radiant temperatures facing and opposite to the stove, respectively).

Case	Sun	Tpr,front	Tpr,back	Tpr,front	Tpr,back
	Living room	Living room	Living room	Kitchen	Kitchen
N°	[Yes-No]	[°C]	[°C]	[°C]	[°C]
1p	No	35.4	26.6	-	-
2p	No	32.3	25.2	-	-
4p	No	36.2	27.5	-	-
2w	No	33.2	28.4	28.9	26.2
4w	No	32.0	27.3	28.8	27.1
5w	No	31.6	26.7	28.0	26.1
7w	No	31.1	25.2	27.2	24.9
8w	No	36.1	27.9	29.1	25.0

Table 6. Measured discharge coefficients (C_d) for the bidirectional flow through the doorway.

Case	Cdv	Cdm	Cdms	Cdes
N°	[-]	[-]	[-]	[-]
1p	0.36	0.35	0.32	0.58
3p	0.40	0.38	0.36	0.61
1w	0.39	0.37	0.35	0.54
2w	0.39	0.38	0.33	0.62
3w	0.41	0.40	0.39	0.62
5w	0.38	0.36	0.35	0.53

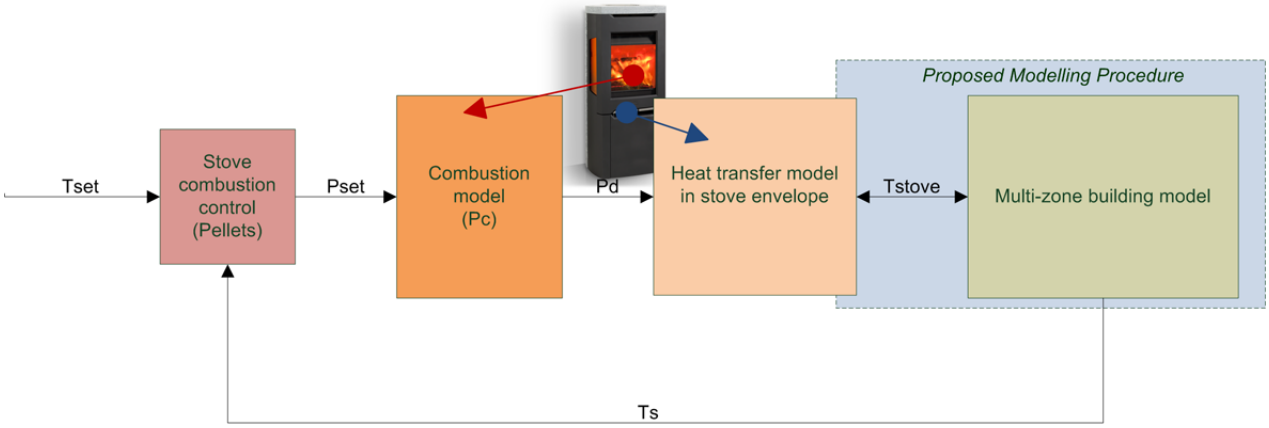

Figure 1. Generic layout of the complete modelling chain to capture the dynamic interaction of a wood stove with a building: the different model components and their interactions are reported, while the scope of the specific modelling procedure proposed in the article is highlighted.

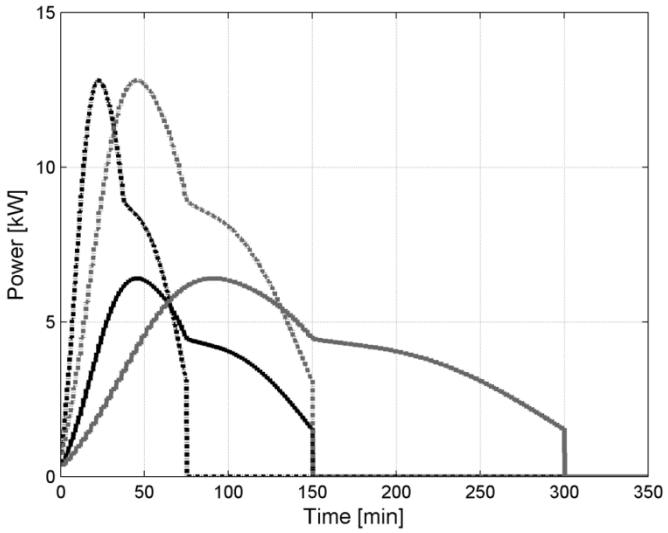

Figure 2. Example of combustion power as a function of time for a 8 kW log stove, from semi-empirical model, Skreiberg et al 2002.: the stove operated at 50% of Pn is shown in solid line while dash-dotted lines are representative of a stove at nominal load; two batches of 10 and 20 kWh are in black and grey, respectively.

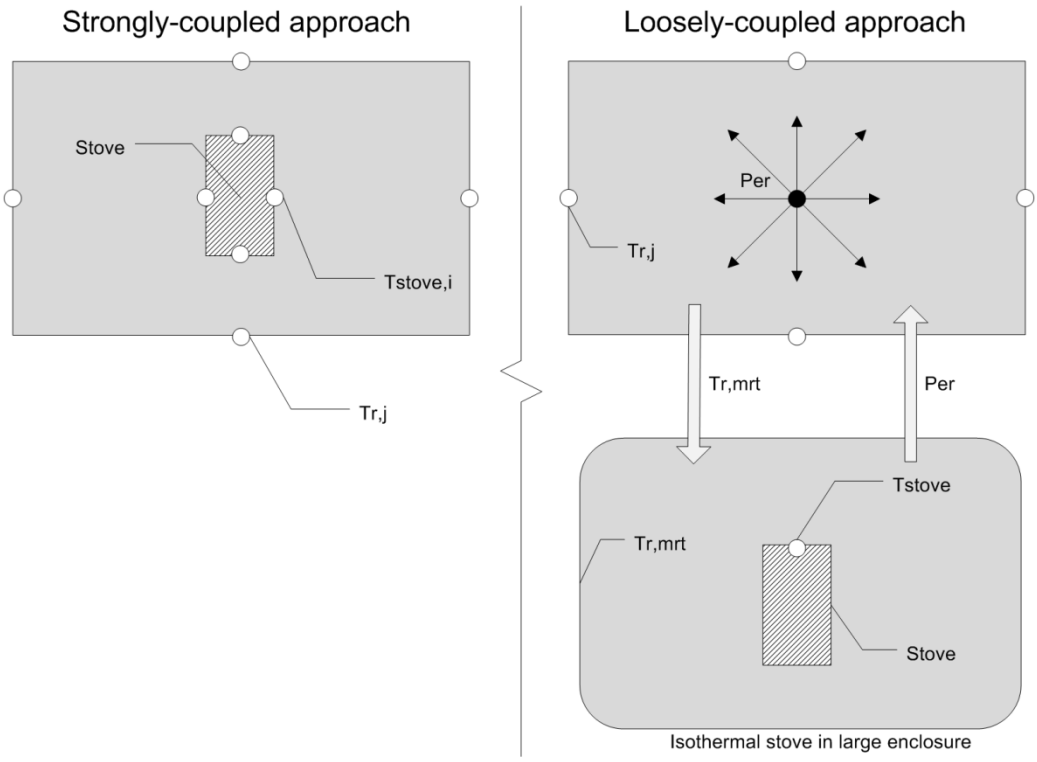

Figure 3. Difference in thermal radiation treatment between the *fully* and l*oosely coupled* approaches.

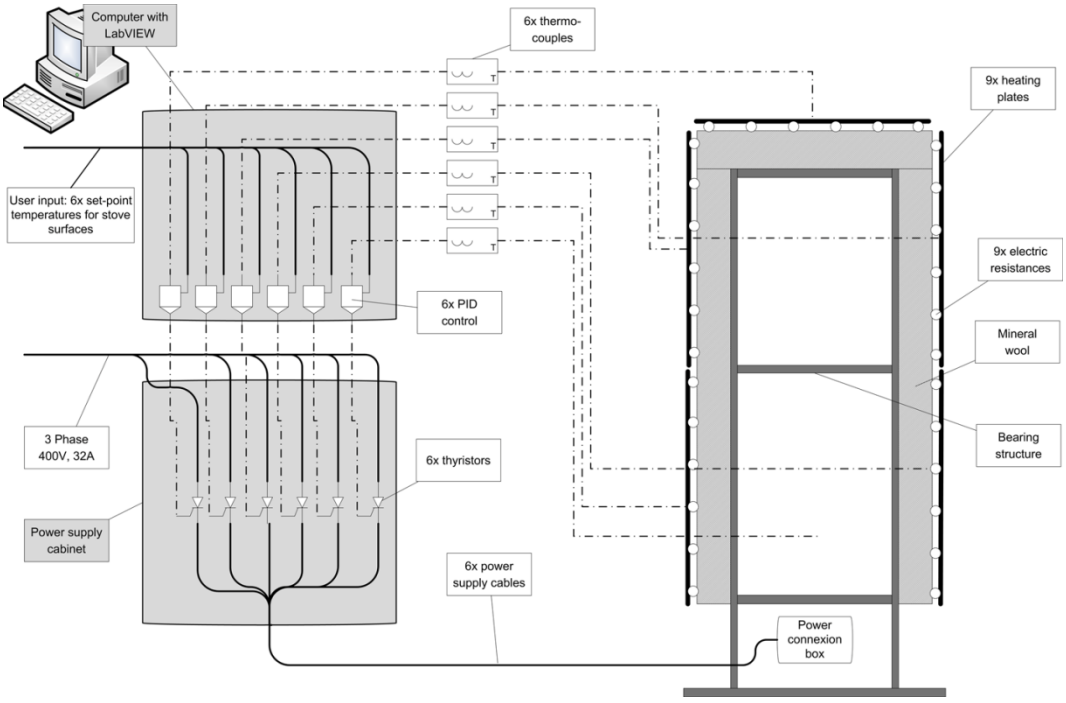

Figure 4. Layout of the movable electric stove experimental setup.

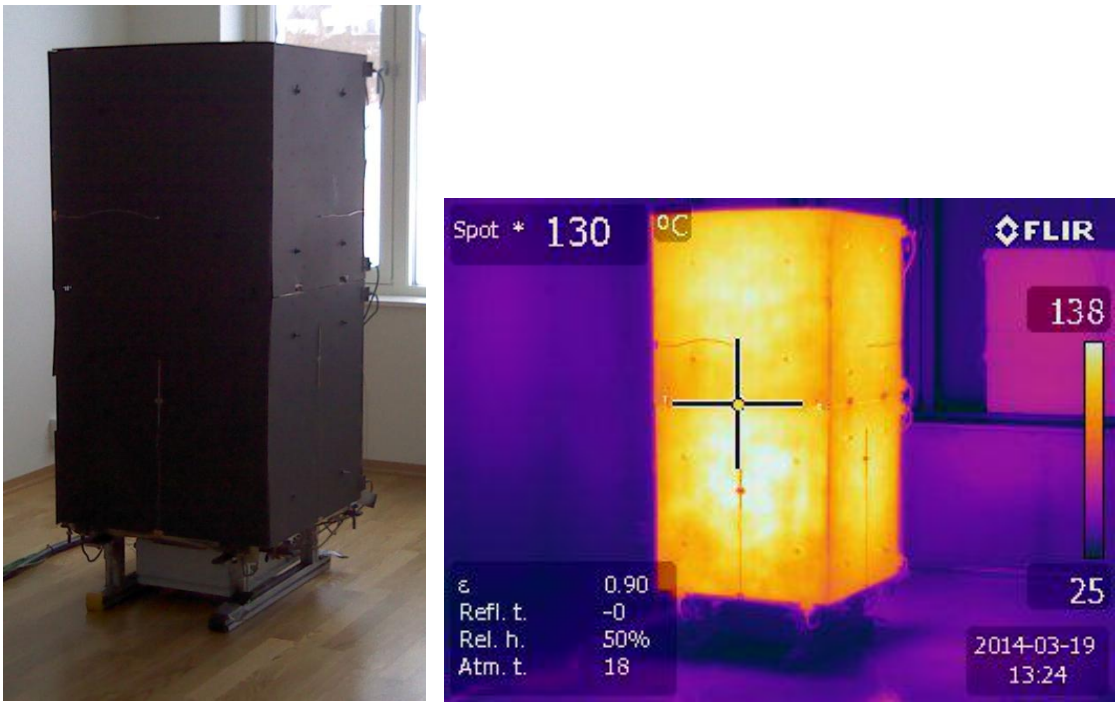

Figure 5. Infrared (IR) picture of the movable stove during operation.

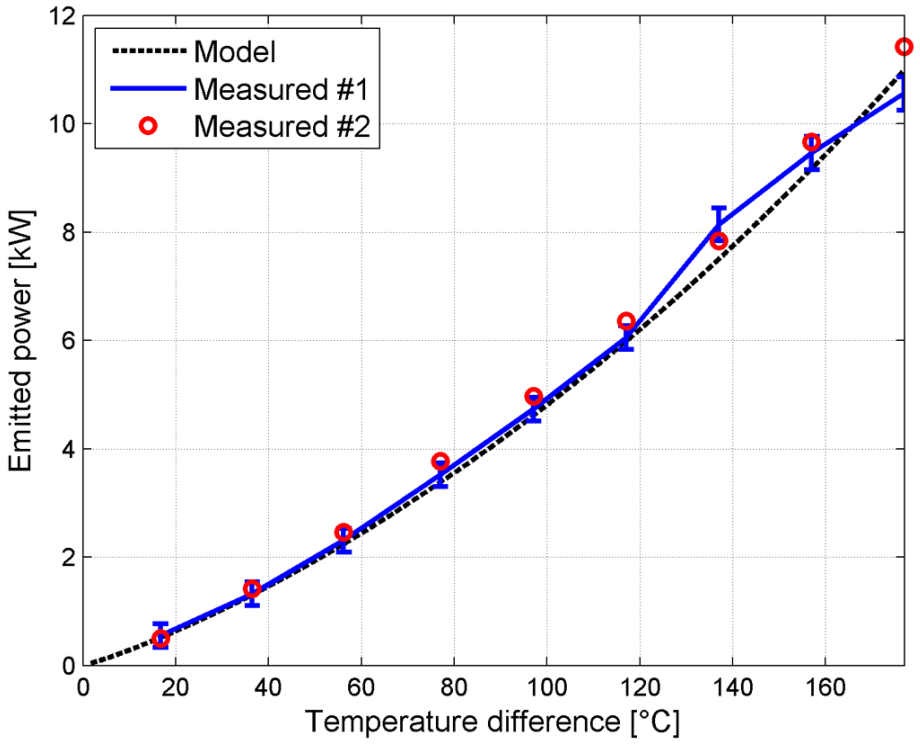

Figure 6. Heating power emitted to the room as a function of the temperature difference between the stove surface (T_{stove}) and the room temperature (T_s): the power emitted by the stove have been measured using two different methods #1 and #2.

Figure 7. Pictures of the building block and sketches of the basement, ground and first floors.

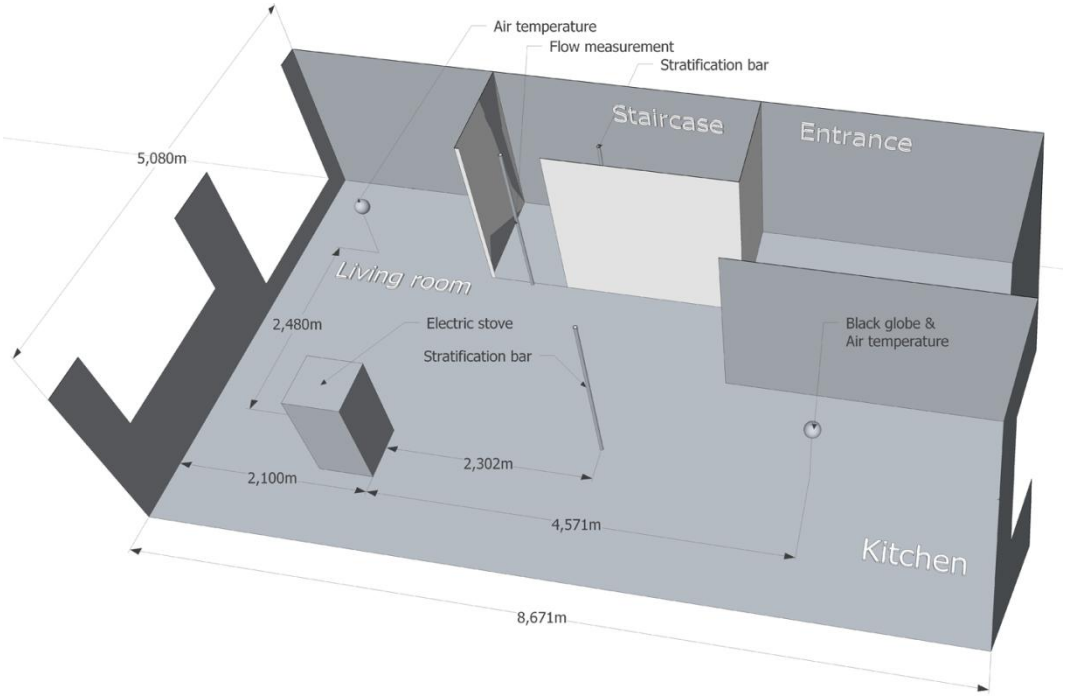

Figure 8. Sketch of the probes and electric stove locations on the ground floor (this also corresponds to the picture 6(b)).

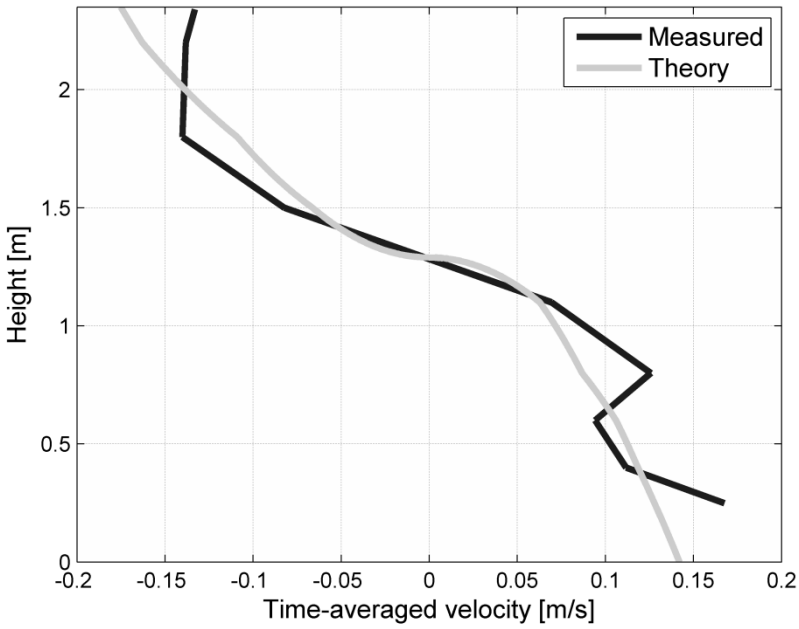

Figure 9. Time-averaged velocity profiles along the door height for test case n°1p.

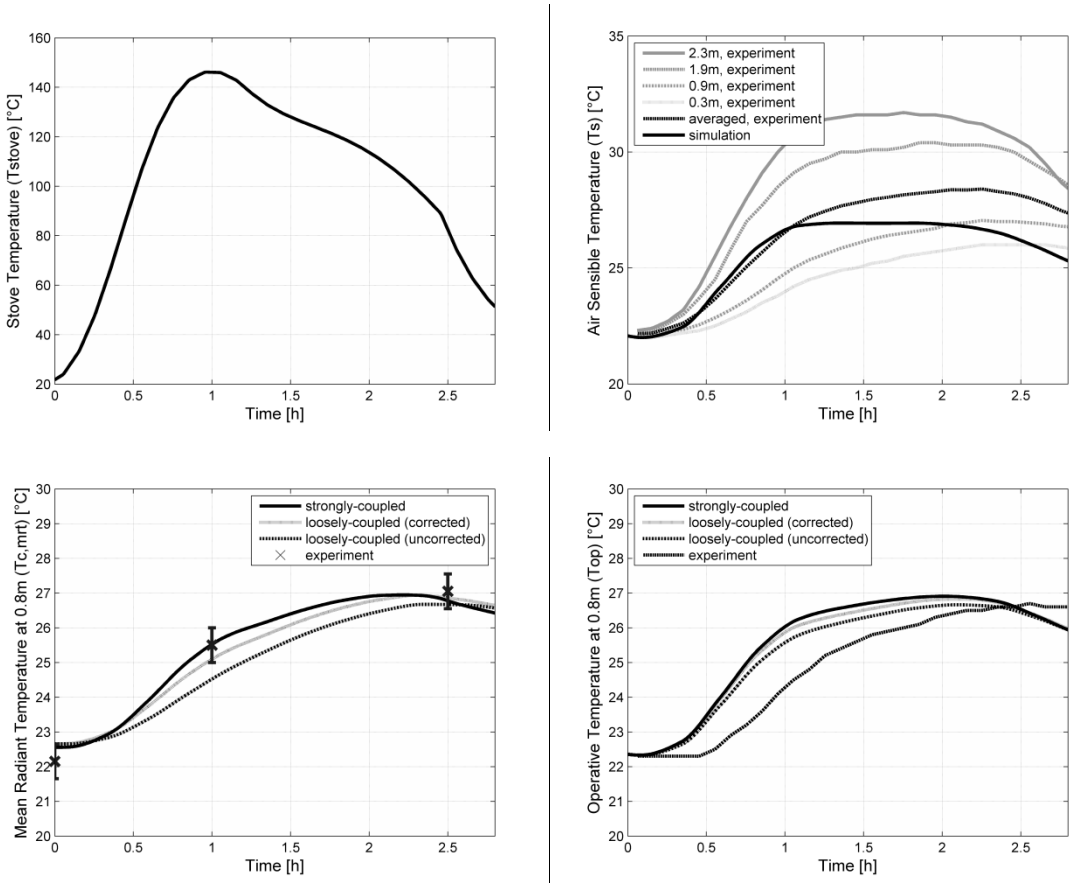

Figure 10. Comparison between field measurements and simulation for the test case n°5w: "corrected/uncorrected" refers to a T_{mrt} which does or does not account for the stove surface temperature.

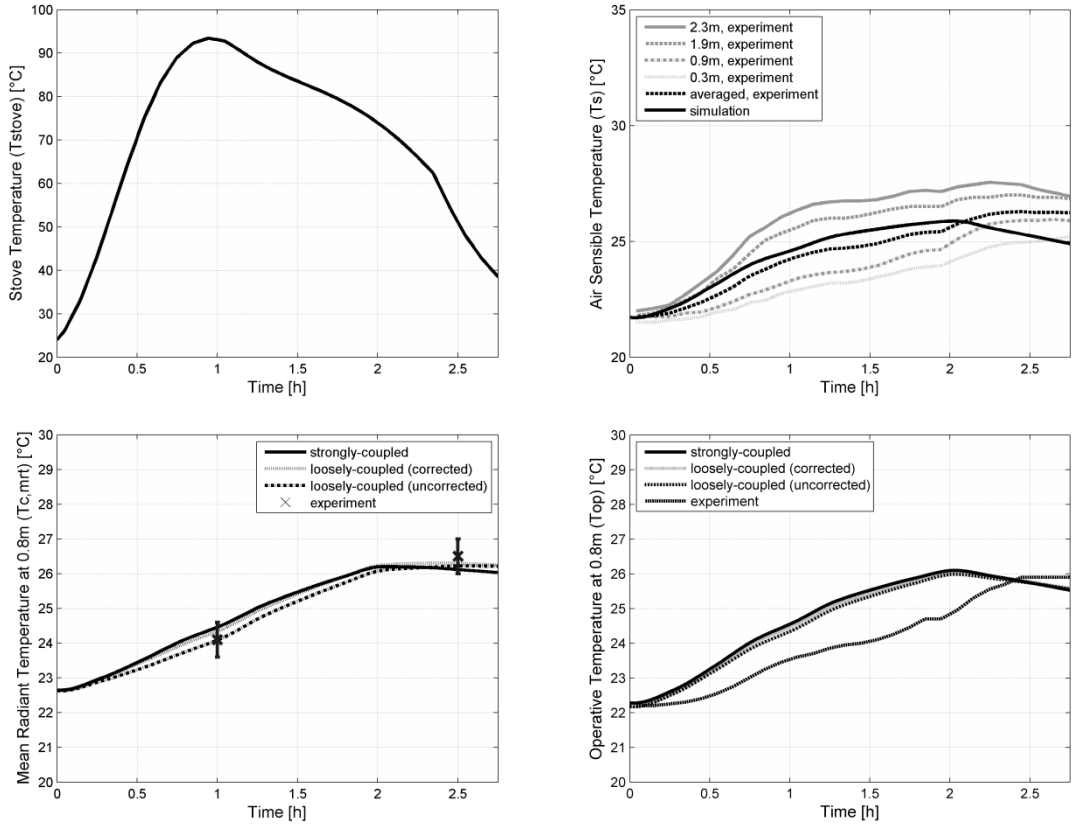

Figure 11. Comparison between field measurements and simulation for the test case n°1w: "corrected/uncorrected" refers to a T_{mrt} which does or does not account for the stove surface temperature.